

(Preprint) AAS 20-088

REVISITING OSIRIS-REX TOUCH-AND-GO (TAG) PERFORMANCE GIVEN THE REALITIES OF ASTEROID BENNU

Kevin Berry,^{*} Kenneth Getzandanner,^{*} Michael Moreau,^{*} Peter Antreasian,[†]
Anjani Polit,[‡] Michael Nolan,[‡] Heather Enos,[‡] and Dante Lauretta[‡]

The Origins, Spectral Interpretation, Resource Identification, and Security–Regolith Explorer (OSIRIS-REx) mission is a NASA New Frontiers mission that launched in 2016 and rendezvoused with the near-Earth asteroid (101955) Bennu in late 2018. Upon arrival, the surface of Bennu was found to be much rockier than expected.¹ The original Touch-and-Go (TAG) requirement for sample collection was to deliver the spacecraft to a site with a 25-meter radius;² however, the largest hazard-free sites are no larger than 8 meters in radius. To accommodate the dearth of safe sample collection sites, the project re-evaluated all aspects of flight system performance pertaining to TAG in order to account for the demonstrated performance of the spacecraft and navigation prediction accuracies. Moreover, the project has baselined onboard natural feature tracking³ instead of lidar for providing the onboard navigation state update during the TAG sequence. This paper summarizes the improvements in error source estimation, enhancements in onboard trajectory correction, and results of recent Monte Carlo simulation to enable sample collection with the given constraints. TAG delivery and onboard navigation performance are presented for the final four candidate TAG sites.

INTRODUCTION

The primary objective of the Origins, Spectral Interpretation, Resource Identification, and Security–Regolith Explorer (OSIRIS-REx) mission is to study the near-Earth asteroid (101955) Bennu and return a pristine regolith sample to Earth.⁴ The spacecraft arrived at Bennu on December 3, 2018, and has been conducting proximity operations to map the entire surface and determine the distribution of regolith and boulders. On a global scale, Bennu’s properties largely match those determined by the pre-encounter astronomical campaign. However, the rocky surface of Bennu was found to have much fewer and smaller patches of boulder-free regions than was originally predicted.^{1,5}

The original requirement on the Flight Dynamics System was to deliver the spacecraft to within 25 m of a given Touch-and-Go (TAG) site, and this requirement was met with over 20% margin across the entire surface of Bennu with a simple lidar-based onboard guidance algorithm.² As surface observations were being made, it was found that the largest hazard-free sites are no larger than 8 m in radius, providing a new challenge for the project to overcome.

^{*} NASA/GSFC, Code 595, 8800 Greenbelt Road, Greenbelt, MD, USA

[†] KinetX, Inc., Space Navigation and Flight Dynamics (SNAFD) Practice, Simi Valley, CA, USA

[‡] Lunar and Planetary Laboratory, University of Arizona, Tucson, AZ, USA

To improve the TAG delivery accuracy, the project decided to switch to the onboard software system called Natural Feature Tracking (NFT)³ for the onboard guidance algorithm that provides the navigation state update during the TAG sequence. Although lidar provides accurate range measurements, it cannot directly provide accurate cross-track information as NFT can. Also, there was a concern that the unexpected degree of albedo heterogeneity^{1,5} would be problematic for the automatic gain controller in the lidar system. Fortunately, NFT had already been developed and implemented as a backup capability.

OVERVIEW OF THE TAG SEQUENCE

The TAG sequence consists of a burn to depart orbit, two burns to target the TAG site position and TAG velocity, the actual TAG event, and then the back-away burn. The original design is detailed in the 2015 paper by Berry et al.², but we are no longer planning on using a circular orbit prior to orbit departure. The TAG sequence now begins in a “frozen orbit” that is slightly offset from the Bennu solar terminator plane. This orbit was designed to balance the perturbations from solar radiation pressure with the low gravity of the asteroid, providing orbit stability over a period of several months.⁶ The frozen orbit is determined by finding an equilibrium solution to the Lagrange planetary equations such that none of the Keplerian orbit parameters evolve over time, with a result that has an eccentricity of roughly 0.15 as is shown in Figure 1.

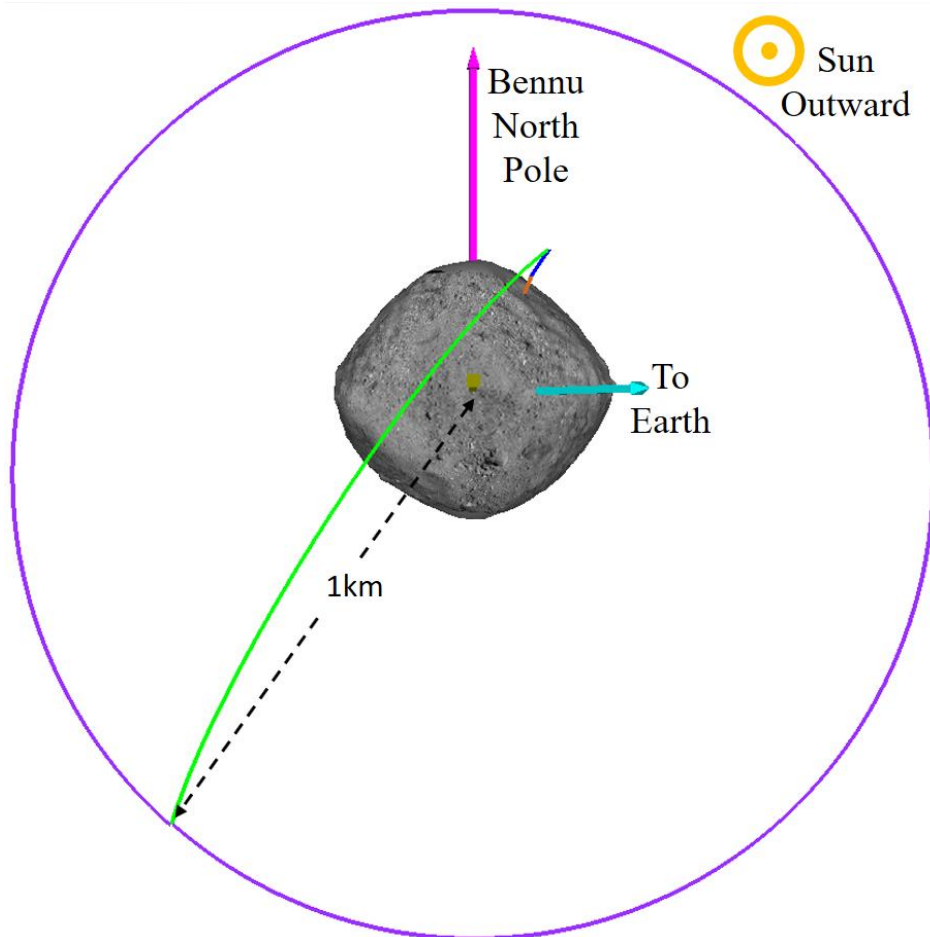


Figure 1. Frozen Orbit (purple) and TAG trajectory (green)

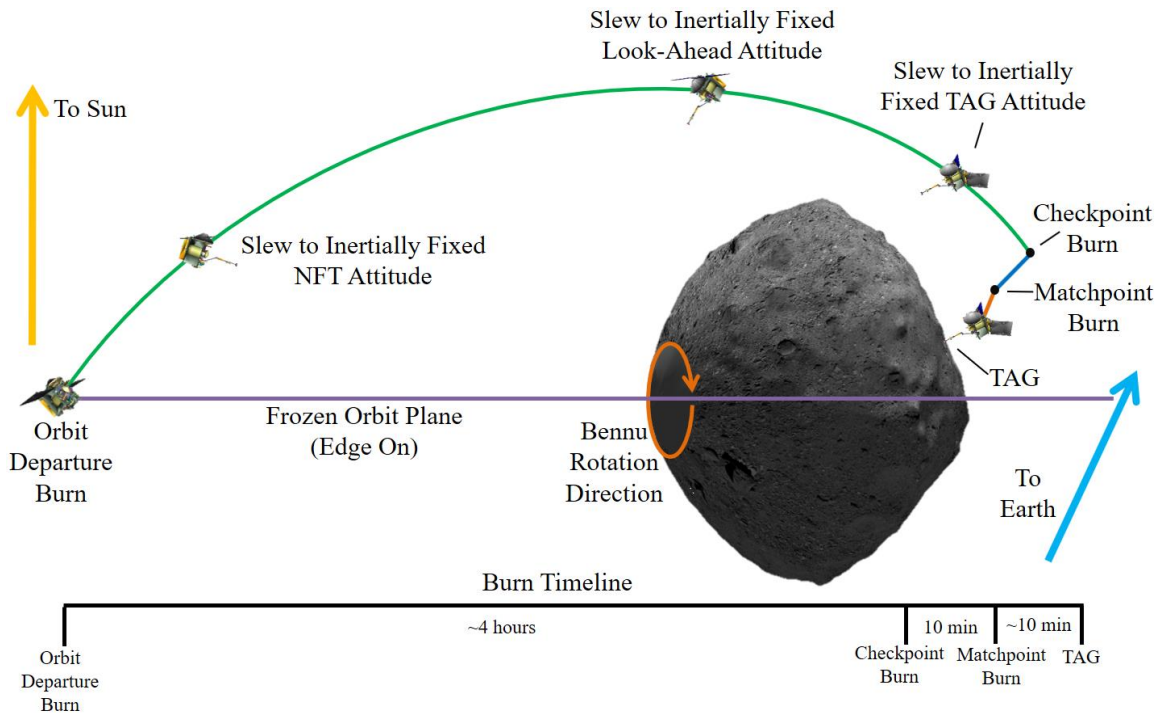


Figure 2. TAG Sequence Viewed Along the Orbit Normal Vector after Orbit Departure

The orbit departure maneuver occurs on the morning side of the asteroid at roughly 1 km from Benu’s center with a latitude that is opposite of the TAG site latitude to optimize the ground track for natural feature tracking. Approximately 4 hours later, the spacecraft arrives at Checkpoint with an altitude of 125 m above the TAG site on a trajectory that is designed to be passively safe, meaning that the spacecraft will not collide with the surface if the next burn does not execute. Checkpoint is where NFT will check its estimate of the trajectory and update the subsequent burns to correct for dispersions. The updated Checkpoint burn is executed, followed by the Matchpoint burn 10 minutes later. Matchpoint occurs at 50 m above the TAG site with a burn that sets the horizontal velocity to match the surface rotation at TAG. This is the final correction to the trajectory, after which the spacecraft will be in a free fall towards the surface until it makes contact at the TAG site with a vertical velocity of -10 cm/s. Since the Checkpoint and Matchpoint burns are executed in the TAG attitude, they are each split into 3 burns and performed sequentially in the 3 axes of the spacecraft body frame. After contact has been made and a sample has been collected, the spacecraft executes a 70 cm/s Backaway burn that is large enough to escape Benu’s gravitational pull in all worst case contact scenarios.

The spacecraft attitudes used during the TAG sequence are all inertially fixed following the orbit departure burn, as shown in Figure 2. The NFT attitude is defined to point the camera in the nadir direction at 1 hour after orbit departure while pointing the solar arrays as close to the Sun as possible. This allows images of the Benu surface to be collected for processing in the NFT Kalman filter. Since the attitude is inertially fixed, the surface would leave the camera field of view if the spacecraft remained in this attitude too long. The final attitude that it needs to be in prior to the Checkpoint burn is the TAG attitude, which aligns the sample collection arm with the TAG site surface normal vector and constrains the other spacecraft axes to ensure communication with Earth via the low gain antenna. An intermediate attitude is needed between the NFT attitude and the TAG attitude to continue to collect surface images, so the spacecraft slews to the Look-Ahead attitude 1 hour before Checkpoint. The Look-Ahead attitude is defined by rotating the TAG attitude by 30

degrees about the negative orbit normal vector, moving the camera field of view closer to nadir and ahead of where it would be in the TAG attitude, hence the name Look-Ahead. The solar array configuration changes throughout the TAG sequence to maintain power, ending with the “Y-wing” configuration in the TAG attitude as shown in Figure 2 to protect the arrays during contact with the surface and the Backaway burn.

In the final descent to the surface, NFT will continue to process images to estimate the time and position where TAG will actually occur. This information can be used to wave-off the TAG attempt by triggering the Backaway burn early to terminate the descent. The original design had this capability limited to a check against a maximum radial distance from the TAG site center, which was intended to be used as a fail-safe against an anomalous event sending our trajectory far off course. In light of the challenges facing the TAG design, the spacecraft team has implemented a new capability that compares the NFT predicted TAG position and its uncertainty to an onboard hazard map and calculates the probability of unsafe contact, triggering a wave-off if that probability is larger than a predetermined threshold. This new capability enables us to safely attempt sample collection at a site that is smaller than the expected delivery ellipse, effectively changing the driving metric from delivery ellipse size to probability of success.

IMPROVED MODELING

As was previously mentioned, the largest hazard-free sites on the Bennu surface are no larger than 8 m in radius, which is much smaller than the 25-m delivery requirement that the mission was designed to accomplish. In addition to making the NFT guidance algorithm prime, it also became necessary to reevaluate all conservative error models and improve performance wherever possible. An exhaustive evaluation was undertaken by the navigation team and the spacecraft team to parameterize observed in-flight performance and determine where predictive uncertainties can be tightened.

Navigation Performance in the Terminator Orbit

Due to the small size and mass of Bennu, it is extremely important for the navigation team to accurately model gravitational forces as well as all non-gravitational forces down to 0.1 nm/s². These forces include the Bennu spherical harmonic gravity model, solar radiation pressure, spacecraft thermal re-radiation pressure, Bennu surface thermal re-radiation pressure, and antenna pressure.^{7,8} Rigorously modeling all of these forces during proximity operations at Bennu resulted in a substantial improvement in the state uncertainty at orbit departure as shown in Table 1.

Table 1. Navigation State Uncertainty at Orbit Departure

	Position Uncertainty (m, 3 σ)			Velocity Uncertainty (mm/s, 3 σ)		
	Radial	Transverse	Normal	Radial	Transverse	Normal
Pre-Launch	12.5	52.6	3.80	3.92	0.506	0.0314
In-Flight	3.63	20.6	0.523	1.58	0.169	0.0785

Maneuver Execution Performance

The pre-launch maneuver execution error model provided by the Lockheed Martin spacecraft team included the effects of a failed thruster for single fault tolerance, as well as conservative assumptions on thruster misalignments, variation between thrusters, accelerometer errors, and errors

in the spacecraft center of gravity. Performing extensive statistical analysis on in-flight performance, they were able to tighten up these errors sources and update their maneuver Monte Carlo analysis to provide greatly improved performance estimates shown in Table 2. These in-flight performance numbers assume that no thrusters have failed, so they will need to be reevaluated in the unlikely event of a thruster failing before TAG. Note that the X, Y, and Z components of the Checkpoint and Matchpoint burns now have varying maneuver execution errors. Since these individual component burns occur sequentially, slosh effects change the expected errors based on when each burn occurs in the sequence. The Checkpoint burn sequence is X-Y-Z, while the Matchpoint burn sequence is Z-Y-X.

Table 2. Maneuver Execution Errors

	Pre-Launch		In-Flight	
	Magnitude Error	Transverse Error	Magnitude Error	Transverse Error
Orbit Departure	RSS(0.3mm/s, 1.5%ΔV)	0.3mm/s+2.5%ΔV	RSS(0.2mm/s, 0.3%ΔV)	0.0mm/s+1.3%ΔV
Checkpoint X	RSS(1.5mm/s, 5.0%ΔV)	1.5mm/s+10%ΔV	RSS(1.3mm/s, 4.4%ΔV)	0.0mm/s+3.0%ΔV
Checkpoint Y	RSS(1.5mm/s, 5.0%ΔV)	1.5mm/s+10%ΔV	RSS(1.3mm/s, 4.4%ΔV)	1.0mm/s+3.5%ΔV
Checkpoint Z	RSS(1.5mm/s, 5.0%ΔV)	1.5mm/s+2.5%ΔV	RSS(1.3mm/s, 4.4%ΔV)	0.5mm/s+1.4%ΔV
Matchpoint X	RSS(1.5mm/s, 5.0%ΔV)	1.5mm/s+10%ΔV	RSS(1.3mm/s, 4.4%ΔV)	1.0mm/s+3.0%ΔV
Matchpoint Y	RSS(1.5mm/s, 5.0%ΔV)	1.5mm/s+10%ΔV	RSS(1.3mm/s, 4.4%ΔV)	1.3mm/s+5.5%ΔV
Matchpoint Z	RSS(1.5mm/s, 5.0%ΔV)	1.5mm/s+2.5%ΔV	RSS(1.3mm/s, 4.4%ΔV)	0.0mm/s+1.2%ΔV

NFT Performance

As a result of the improvements in navigation and maneuver execution performance, the NFT team saw a reduction in the Checkpoint prediction uncertainty. Since NFT is running a Kalman filter, initializing it with a smaller covariance after the orbit departure burn results in a more accurate trajectory estimate onboard, as is shown in Table 3. The actual performance varies across the possible TAG sites, so the numbers shown here are bounding. In the final TAG design, these NFT performance estimates will be improved further based on the feature availability in the images expected on the specific TAG trajectory.

Table 3. NFT State Uncertainty at Checkpoint

	Position Uncertainty (m, 3σ)			Velocity Uncertainty (mm/s, 3σ)		
	Radial	Transverse	Normal	Radial	Transverse	Normal
Pre-Launch	3.0	3.0	3.0	3.0	3.0	3.0
In-Flight	2.1	2.1	2.1	2.9	2.9	2.9

In addition to the Checkpoint prediction improvement, the spacecraft team developed a flight software patch that enables an NFT wave-off assessment against a hazard map. Since that assessment uses the NFT uncertainty calculated onboard at a range of 5 m from the surface on its TAG position estimate to calculate the probability of unsafe contact, we needed a bounding uncertainty to use in the comparison of the probability of success between the various TAG sites being analyzed. The NFT team determined the uncertainty in the TAG position estimate at the time of the final onboard solution and provided a conservative estimate of 1.27 m (3σ) to be used in the site selection process, with an expectation that this will also be improved upon for the selected site.

FINAL FOUR CANDIDATE SAMPLE SITES

The site selection process began shortly after arrival in December of 2018. Global maps were created for Deliverability, Safety, Sampleability, and Science Value, which were all compared to determine the regions of interest for the various teams to focus on. This process is what highlighted the need for the performance improvements discussed in the previous sections, resulting in additional observations of the surface and several iterations with the site selection board as we learned more and refined our maps. The regions of interest were exhaustively analyzed and compared until they were narrowed down to the “Sweet Sixteen”, followed by the “Elite Eight”. In August of 2019, the project announced the selection of the “Final Four” sites shown in Figure 3 and Figure 4.



Figure 3. Locations of the Final Four TAG Sites on Bennu. Image credit: NASA/University of Arizona

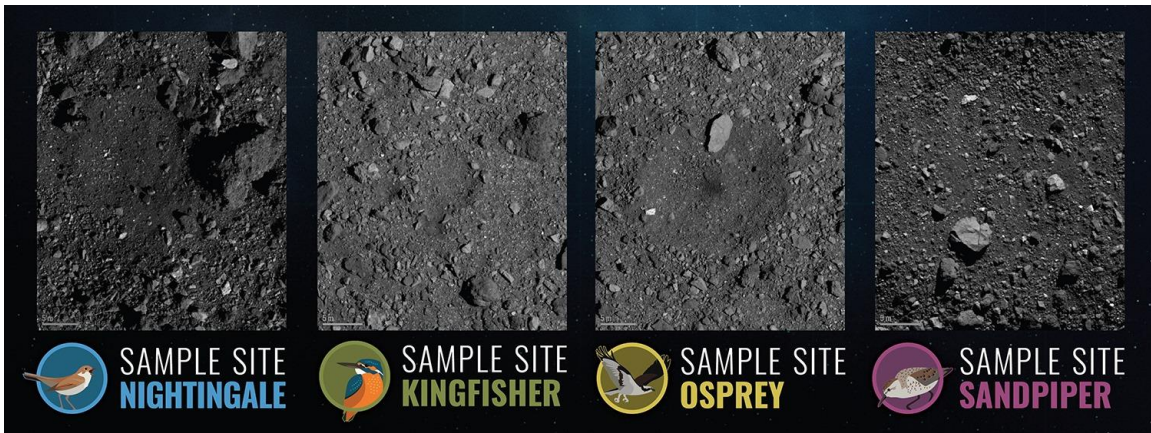


Figure 4. Images of Each of the Final Four TAG Sites. Image credit: NASA/University of Arizona

MONTE CARLO SIMULATION

A thorough Monte Carlo analysis is needed to determine the combined effects of all error sources propagated with non-linear dynamics along with the NFT guidance update to the Checkpoint and Matchpoint burns. The trajectory design and targeting in this analysis is performed with STK (Systems Tool Kit) by Analytical Graphics, Inc. MATLAB (by MathWorks, Inc.) is used to drive the Monte Carlo analysis by automating the inputs to the STK scenario and applying the various perturbations to the nominal trajectory. A detailed description of the algorithms can be found in Berry et al.²

Orbit Departure Dispersions

The dispersions following the orbit departure burn are shown in Table 4 for the Final Four TAG sites, along with the range of dispersions that were seen in the Monte Carlo analysis that was performed before the mission launched. In general, the dispersions have been cut in half with the improved modeling described previously. These dispersion are used to initialize the NFT filter.

Table 4. Trajectory Dispersions after Orbit Departure Burn

	Position Dispersions (m, 3σ)			Velocity Dispersions (mm/s, 3σ)		
	Radial	Transverse	Normal	Radial	Transverse	Normal
Pre-Launch	14 - 15	11 - 36	40 - 52	4.2 - 4.4	1.5 - 1.7	1.3 - 1.6
Nightingale	4.65	3.29	19.7	1.78	0.738	0.591
Kingfisher	4.85	3.37	20.2	1.79	0.729	0.600
Osprey	4.83	3.67	20.1	1.79	0.737	0.609
Sandpiper	4.69	8.10	19.0	1.74	0.712	0.528

Checkpoint Dispersions

Propagating the dispersed trajectories to Checkpoint results in an elongation of the covariance in the transverse direction. The Checkpoint dispersions shown in Table 5 represent the range of trajectory errors that the NFT guidance algorithm will need to correct for with the Checkpoint and Matchpoint burn update. This dramatic improvement in dispersions result in a more accurate NFT estimate and a more accurate TAG delivery.

Table 5. Trajectory Dispersions before Checkpoint Burn

	Position Dispersions (m, 3σ)			Velocity Dispersions (mm/s, 3σ)		
	Radial	Transverse	Normal	Radial	Transverse	Normal
Pre-Launch	28 - 37	68 - 120	9.1 - 12	17 - 29	7.5 - 8.8	8.5 - 11
Nightingale	9.89	50.4	3.66	12.0	3.39	4.69
Kingfisher	12.9	48.1	3.22	11.1	3.33	4.14
Osprey	12.3	47.1	3.36	11.4	3.24	4.29
Sandpiper	10.9	42.0	2.98	10.7	2.96	4.21

TAG Dispersions

Continuing the Monte Carlo runs to the surface, the TAG dispersions in Table 6 show that we were able to reduce the pre-launch position errors of 17–20 m down to 5.7–8.1 m. The velocity dispersions are also much smaller, giving us more margin against the 20 mm/s maximum horizontal and vertical velocity requirements that the spacecraft was designed to. The next section will show the TAG position error ellipses overlaid on each of the TAG sites and what the resulting probabilities of success are.

Table 6. TAG Dispersions

	Position Dispersions (m, 3σ)	Horizontal Velocity Dispersions (mm/s, 3σ)	Vertical Velocity Dispersions (mm/s, 3σ)
Pre-Launch	17 - 20	12 - 15	9.4 - 15
Nightingale	8.12	6.64	6.95
Kingfisher	5.89	5.03	7.54
Osprey	5.66	4.56	6.39
Sandpiper	7.29	6.47	5.57

PROBABILITY OF SUCCESS

For each TAG site, a hazard map is generated that determines the regions where contact may be unsafe. Since the spacecraft can tip over up to 25 degrees during contact, larger boulders and hills present tip-over hazards and backaway hazards if TAG occurs adjacent to one and the spacecraft tips toward it before the Backaway burn starts. The hazard maps shown in this section, along with the corresponding success probability calculations, are based on tip-over and backaway hazards only. Future work will include adding rocks and boulders that could be hazardous for the sample collection head to make contact with, which may reduce the success probabilities shown.

On a given trajectory down to the TAG site, NFT will predict the actual TAG position with an uncertainty that is expected to be less than 1.27 m (3σ). The flight software takes that predicted TAG position and covariance and integrates the corresponding 2-dimensional probability density function against the hazard map to determine the probability of unsafe contact. If that probability is larger than a configurable threshold, NFT will trigger a wave-off to protect the spacecraft, resulting in an early Backaway burn at 5 meters altitude. In this analysis, the threshold used for a given site is derived based on a 0.5% total probability of unsafe contact across the entire site area, which was chosen to give us margin against the 1% requirement. The final probability of unsafe contact will be determined just prior to TAG implementation.

To determine the probability of success for each TAG site, the delivery ellipse is used to determine the probability of contact with every facet in the hazard map. The NFT wave-off assessment is performed for a trajectory that is estimated to make contact with each individual facet, and facets that triggered a wave-off are summed to determine the total probability of wave-off. The probability of success is the probability that the spacecraft proceeds to the surface without a wave-off and that there isn't any unsafe contact, which is shown in Equation (1).

$$P_{Success} = 1 - P_{Wave-Off} - P_{Unsafe} \quad (1)$$

Figure 5 shows the 3σ delivery ellipses colored blue for each site overlaid on the hazard maps, along with the three probabilities previously mentioned. The facets of the hazard maps are colored according to the following scheme:

Red & Yellow: NFT wave-off

- Probability of contact with hazard \geq threshold
- Red facets are potential hazards
- Yellow facets are close enough to red to trigger wave-off

Green & Pink: No NFT wave-off

- Probability of contact with hazard $<$ threshold
- Green facets are free of hazards and are considered successful TAG attempts
- Pink facets are hazards too small to trigger wave-off and represent unsafe contacts

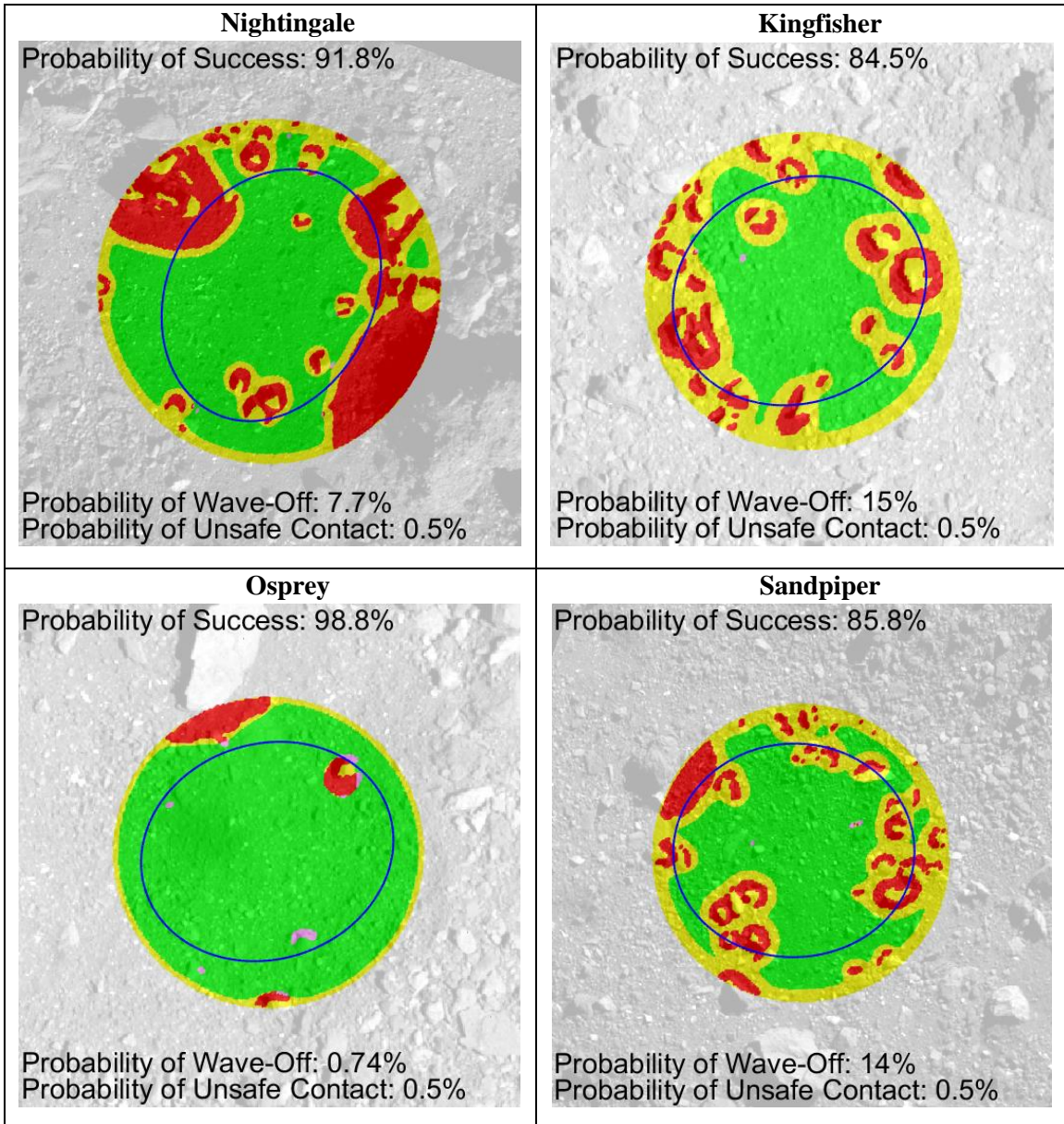


Figure 5. TAG Deliverability & Hazard Maps

CONCLUSIONS

To meet the challenges presented by the unexpectedly rocky landscape of Benu, the OSIRIS-REx team was able to modify the prelaunch TAG design through performance improvements and enhancements to the NFT estimation algorithms. Adding the NFT wave-off capability allowed the delivery error metric to be changed to a configurable probability of success, which made it possible to easily rank each site for comparison with the other site selection criteria. On December 12 of 2019, the project announced the selection of Nightingale as the primary TAG site due to its abundance of fine-grained material and its relatively high probability of successful collection of at least 60 g of regolith (the mission level-1 requirement). The backup site was selected to be Osprey, which has less fine-grained materials but a higher probability of surface contact (the minimum mission success criterion).

ACKNOWLEDGEMENTS

The OSIRIS-REx flight team has performed extensive analysis and parameterization to improve the performance of the TAG design, making sample collection possible in the uncooperative rubble pile that is Benu. Any TAG attempt would have been unacceptably perilous without the meticulous work of the navigation team comprised of engineers from KinetX, Inc., and NASA Goddard Space Flight Center, and the spacecraft team at Lockheed Martin Space, with special emphasis on GNC and NFT analysis provided by Curtis Miller, Dale Howell, and Ryan Olds. Additionally, the hazard maps provided by David Lorenz at Goddard Space Flight Center were crucial for this analysis. This material is based upon work supported by NASA under Contracts NNG13FC02C and NNM10AA11C issued through the New Frontiers Program.

REFERENCES

- ¹ D. S. Lauretta, D. N. DellaGiustina et al., The unexpected surface of asteroid (101955) Benu. *Nature* 568, 55–60 (2019).
- ² K. Berry, P. Antreasian, M. Moreau, A. May, B. Sutter, “OSIRIS-REx Touch-And-Go (TAG) Navigation Performance,” *Proceedings of the 38th Annual Guidance and Control Conference*, 2015. AAS 15-125.
- ³ R. Olds, A. May, C. Mario, R. Hamilton, C. Debrunner, K. Anderson, “The Application of Optical Based Feature Tracking to OSIRIS-REx Asteroid Sample Collection.” *Proceedings of the 38th Annual Guidance and Control Conference*, 2015. AAS 15-114.
- ⁴ D. S. Lauretta, et al. "OSIRIS-REx: Sample Return from Asteroid (101955) Benu," *Space Sci. Rev.* 212, 925–984, 2017.
- ⁵ D. N. DellaGiustina, J. P. Emery, et al. "Properties of rubble-pile asteroid (101955) Benu from OSIRIS-REx imaging and thermal analysis," *Nat. Astron.* 3, 341–351, 2019.
- ⁶ D. R. Wibben, A. Levine, S. Rieger, J. V. McAdams, P. Antreasian, J. Leonard, M. Moreau, D. S. Lauretta, “OSIRIS-REx Frozen Orbit Design and Flight Experience,” *AIAA/AAS Astrodynamics Specialist Conference*, AAS 19-677, 2019.
- ⁷ J. M. Leonard, J. L. Geeraert, B. R. Page, A. S. French, P. G. Antreasian, C. D. Adam, D. R. Wibben, M. C. Moreau, D. S. Lauretta, “OSIRIS-REx Orbit Determination Performance During The Navigation Campaign,” *AIAA/AAS Astrodynamics Specialist Conference*, AAS 19-714, 2019.
- ⁸ J. L. Geeraert, J. M. Leonard, P. W. Kenneally, P. G. Antreasian, M. C. Moreau, D. S. Lauretta, “Osiris-Rex Navigation Small Force Models,” *AIAA/AAS Astrodynamics Specialist Conference*, AAS 19-717, 2019.